Electronic Supplementary Information:

Effects of Confinement, Surface-Induced Orientations and Strain on Dynamical Behaviors of Bacteria in Thin Liquid Crystalline Films

Peter C. Mushenheim,[a] Rishi R. Trivedi,[b] Susmit Singha Roy,[c] Michael S. Arnold,[c] Douglas B. Weibel[b] and Nicholas L. Abbott*[a]

[a]*Department of Chemical and Biological Engineering, University of Wisconsin-Madison, 1415 Engineering Drive, Madison, WI, 53706, USA. Fax: +1 608-262-5434; Tel: +1 608-265-5278*

[b]*Department of Biochemistry, University of Wisconsin-Madison, 433 Babcock Drive, Madison, WI, 53706, USA.* Fax: +1 608-265-0764; Tel: +1 608-890-1342

[c]*Department of Materials Science and Engineering, University of Wisconsin-Madison, 1509 University Avenue, Madison, WI, 53706, USA.* Fax: +1 608-262-8353; Tel: +1 608-262-3863

*Correspondence: abbott@engr.wisc.edu

Supplementary Text

Calculation of the rotational drag coefficient for vegetative *P. mirabilis* cells

Modeling vegetative *P. mirabilis* cells as prolate spheroids with semi-major axis a and semi-minor axis b, we estimated the frictional drag coefficient associated with the rotation of the cell around one of its minor axes using the expression $f_r = \frac{4(1-p^4)}{3p^2[aS(2-p^2)-2]} C_o$.[1] In this expression, $p = b/a$, $S = \frac{2}{a}(1-p^2)^{-1/2} \ln\left[\frac{\left[1+(1-p^2)^{1/2}\right]}{p}\right]$, and $C_o = 8\pi a^3 p^2 \eta$ is the coefficient for rotational frictional drag for a sphere with a volume equal to the volume of the ellipsoid. Employing a = 1.5 μm, b = 0.5 μm, and an effective viscosity of $\eta \sim 0.7$ Pa s for the nematic DSCG phase, we estimate $f_r \sim 1.5 \times 10^{-17}$ kg m^2 s^{-1}.

Measurement of the angle of alignment adopted by gyrating vegetative bacteria near graphene-coated substrates

Videos (200 frames long) of vegetative cells gyrating near graphene-coated substrates in uniform homeotropic and hybrid films were collected at different planes of focus separated by 1 μm. The Mosaic ParticleTracker 2D/3D plugin[2] for ImageJ then was used to plot trajectories of the approximately circular cross-sections of the gyrating cells, as depicted in Fig. S5. By determining the average radius of these trajectories collected for an individual gyrating cell at different planes of focus, trigonometric relations could be used to estimate the average angle (ϕ in Fig. S5) formed between the long axis of the vegetative cell and the surface normal.

Estimation of E_{cell} for swarm cells dispersed in a hybrid LC film

To estimate the energetic cost (E_{cell}) of bending a swarm cell of length L in a hybrid LC film of thickness d in the limit of $L > d$, we model the cell as a rod-shaped shell that has thickness w and radius R and use $E_{cell} = \frac{1}{2} E I L_{bend} \kappa^2$.[3] In this expression, *E* is the Young's modulus, I is the second moment of inertia, L_{bend} is the arc length of the bent cell, and κ is the mean curvature of the cell.[3] For a thin, hollow cylinder of thickness w, $I = \frac{1}{4}\pi[R^4 - (R - b)^4] \approx \pi R^3 w$.[4] We assume that if a swarm cell deforms such that its orientation is always parallel to the local director in a LC film of thickness d with hybrid anchoring conditions, the mean curvature of the deformed segment of the swarm cell is given by $\kappa \sim \frac{1}{d}$. Given this curvature, the deformed length of the swarm cell in the hybrid film (in which the out-of-plane orientation of the LC rotates by $\pi/2$ going from the graphene-coated substrate to the bare glass substrate) is $L_{bend} \sim \frac{\pi}{2} d$ (see Fig. S6). Inserting these expressions into the equation for E_{cell}, we arrive at $E_{cell} = \frac{\pi^2 R^3 w E}{4d}$. Employing typical values in our system of R ~ 0.5 μm and d ~ 18 μm, an estimate of the thickness of the peptidoglycan layer of *P. mirabilis* (which imparts rigidity to the cell body) of w ~ 10 nm[5], and an estimate for the Young's modulus of the highly flagellated *P. mirabilis-flhDC* swarm cell of $E \sim 8.743 \times 10^4$ Pa (personal communication from Weibel lab), we estimate $E_{cell} \sim 1 \times 10^{-17}$ J.

Gyration of vegetative *P. mirabilis* cells in hybrid LC films

We found that vegetative *P. mirabilis* cells dispersed in hybrid films also had a tendency to become dynamically positioned near the graphene-coated substrate, similar to the case of homeotropic LC films described in the main text. As a result, we observed that over

the course of an experiment, cells dispersed in hybrid LC films tended to accumulate near the graphene-coated substrate. Each cell positioned near the graphene-coated substrate gyrated about an axis normal to the substrate with a handedness matching that of its rotating flagella bundle (Video S13). However, while we measured the angular velocity of the cell bodies to be comparable to that measured in homeotropic films ($\sim 1 - 2$ rev/s), we determined the cell body to commonly deviate at larger angles (up to 6°) away from the surface normal. We hypothesize that the combined effects of changes in the orientation of the far-field director profile over the length of the cell body and bending of the bacterial flagella due to the bend and splay in the LC are likely responsible for the pronounced deviation of the orientation of the cell body away from the surface normal measured in hybrid films.

Supplementary References

1. S. H. Koenig, *Biopolymers*, 1975, **14**, 2421-2423.
2. I. F. Sbalzarini and P. Koumoutsakos, *Journal of Structural Biology*, 2005, **151**, 182-195.
3. L. D. Landau and E. M. Lifshitz, *Theory of Elasticity*, Pergamon Press, 3rd edn., 1986.
4. S. Wang, H. Arellano-Santoyo, P. A. Combs, and J. W. Shaevitz, *Proceedings of the National Academy of Sciences*, 2010, **107**, 9182-9185.
5. J.-P. Martin, J. Fleck, M. Mock, and J.-marie Ghuysen, *European Journal of Biochemistry*, 1973, **38**, 301-306.
6. A. C. Ferrari, J. C. Meyer, V. Scardaci, C. Casiraghi, M. Lazzeri, F. Mauri, S. Piscanec, D. Jiang, K. S. Novoselov, S. Roth, and A. K. Geim, *Physical Review Letters*, 2006, **97**, 187401.

Supplementary Figures

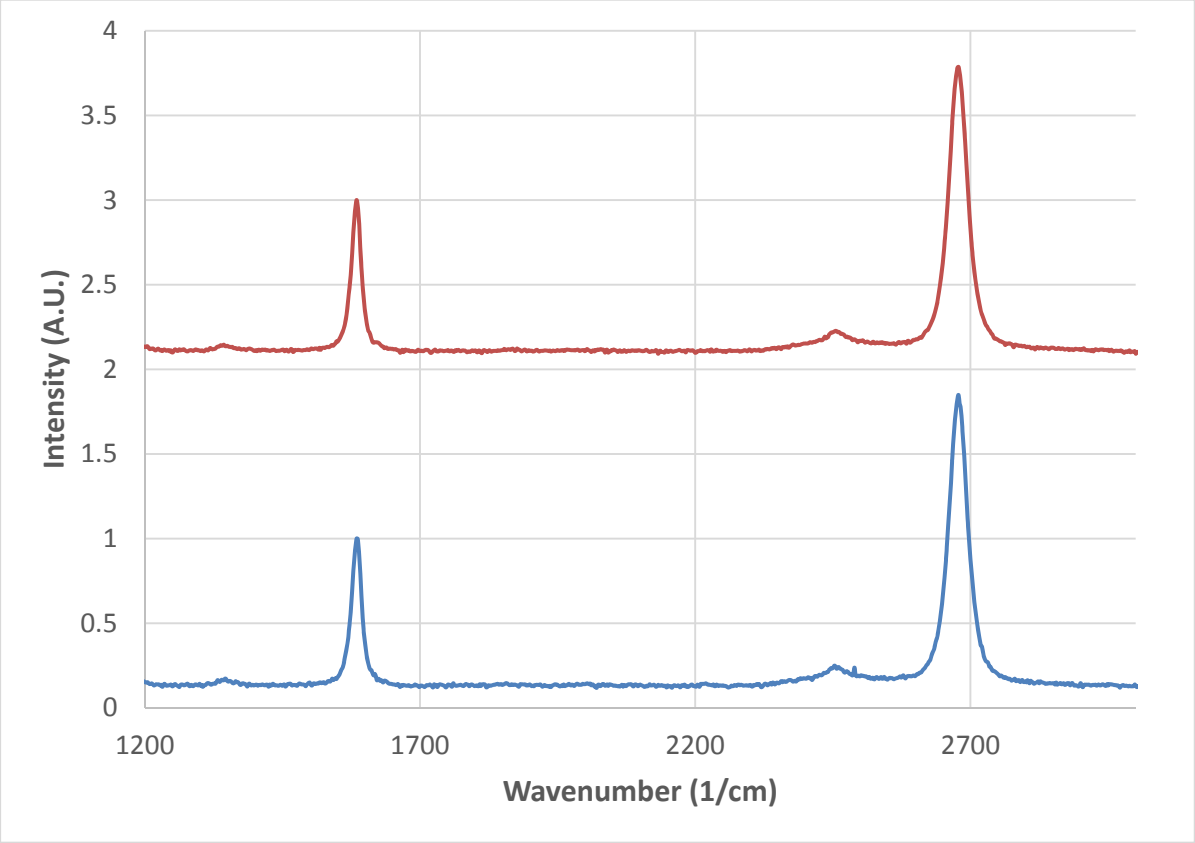

Fig. S1 Spatially-averaged Raman spectra (normalized to the G-band intensity) of a graphene-coated substrate collected both before (blue) and after (red) contact with a 15 wt% DSCG solution for 30 min. The DSCG solution was removed from the surface of the graphene-coated substrate before the second spectrum was collected. A typical Raman spectra for graphene consists of three major bands, namely the D, G and 2D bands at ~1347 cm^{-1}, ~1585 cm^{-1} and 2680 cm^{-1} (for a 532 nm excitation wavelength).[6] In our spectra, the ratio of $I_{2D}/I_G > 1$ confirms the presence of a monolayer of graphene.[6] In addition, the ratio of I_D/I_G is directly proportional to the defect density, with values < 0.1 considered to indicate high quality graphene monolayers grown via chemical vapor deposition (CVD). In our spectra, taken both before and after application of the DSCG solution, we calculated I_D/I_G to be ~ 0.04. This indicates (i) a very low defect density in the as-manufactured graphene layer and (ii) that no additional defects were introduced during the application and removal of the LC.

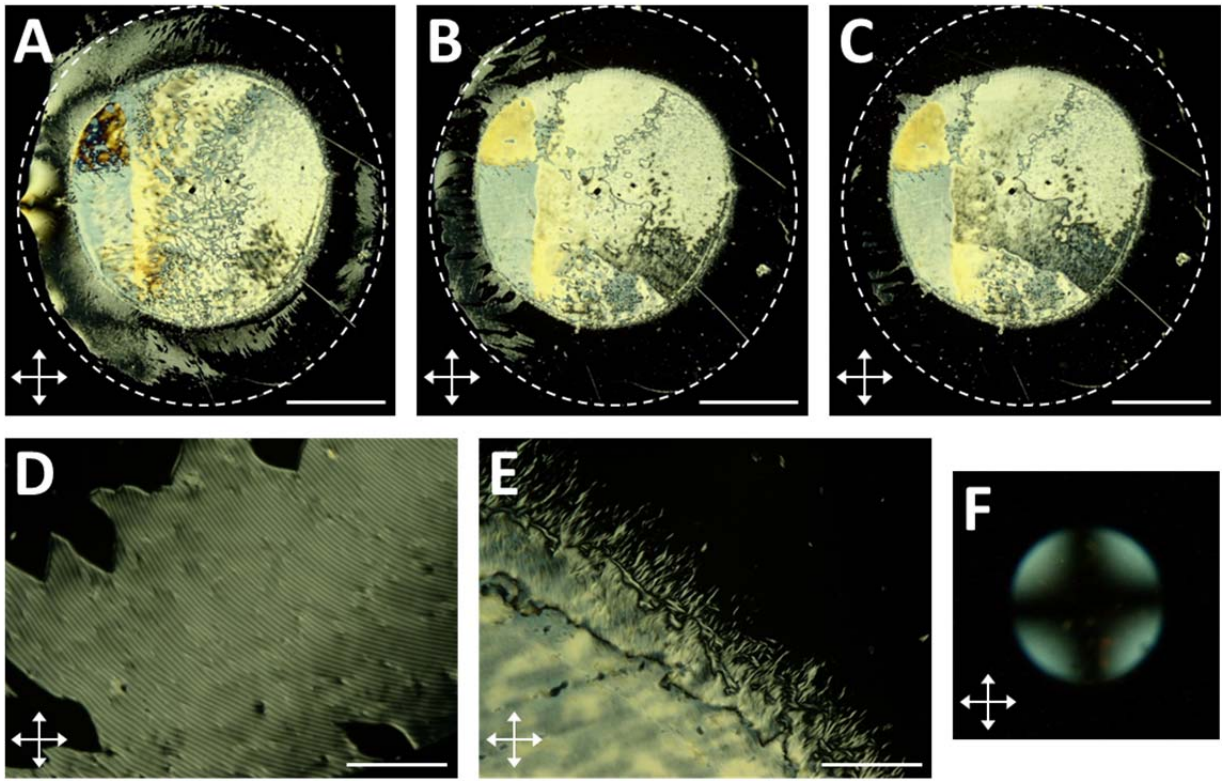

Fig. S2 Evolution of homeotropic orientation in a nematic phase DSCG film. (A-C) Polarized light (crossed polars) micrographs of nematic phase DSCG film (~ 18 μm thick) confined between two graphene-coated substrates taken (A) 20 min, (B) 60 min, and (C) 120 min after preparation of the optical imaging chamber. Dotted white lines superimposed on the images indicate the approximate extent of the LC film. The optical imaging chamber was prepared by sandwiching 1.2 μL of DSCG in the nematic phase between the graphene-coated substrates and sealing with epoxy, using Mylar spacers to set the film thickness. Regions of the LC film in an outer annulus of the film transition to a homeotropic orientation over the initial 120 min and retain this homeotropic orientation for days following. The central region of the film (even after days) was not observed to transition to a homeotropic orientation. (D) Polarized light (crossed polars) micrograph of the transient stripe texture observed in the outer annulus of the LC film as the LC transitions to a uniform homeotropic orientation. Image acquired 25 min after preparation of the optical imaging chamber. (E) Polarized light (crossed polars) micrograph of the transition region observed between the outer annulus exhibiting homeotropic orientation and the inner region that does not. Image acquired 37 min after preparation of the optical imaging chamber. (F) Conoscopic image acquired in the outer annulus of DSCG, confirming uniform homeotropic orientation. Image acquired 70 min after preparation of the optical imaging chamber. Scale bars in A-C = 2 mm; scale bars in D,E = 5 μm.

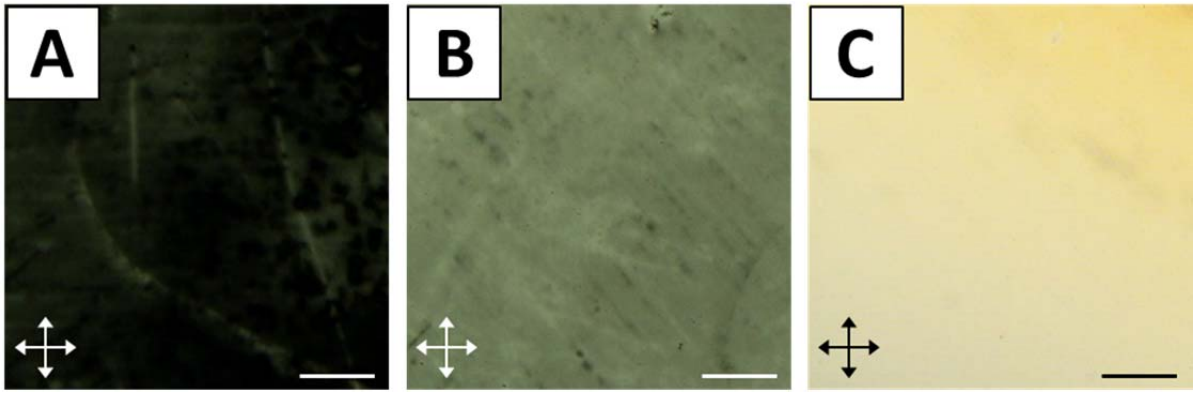

Fig. S3 (A,B) Polarized light (crossed polarizers) micrographs of a region of a hybrid anchored LC film (~ 18 μm thick) exhibiting approximately uniform azimuthal alignment. The sample is rotated such that the direction of azimuthal alignment of the LC is oriented either (A) parallel or (B) 45° relative to the orientation of one of the polarizers. (C) Polarized light (crossed polarizers) micrograph of a uniform planar LC film (~ 18 μm thick) in which the director is oriented 45° relative to the orientation of one of the polarizers. Scale bars = 200 μm.

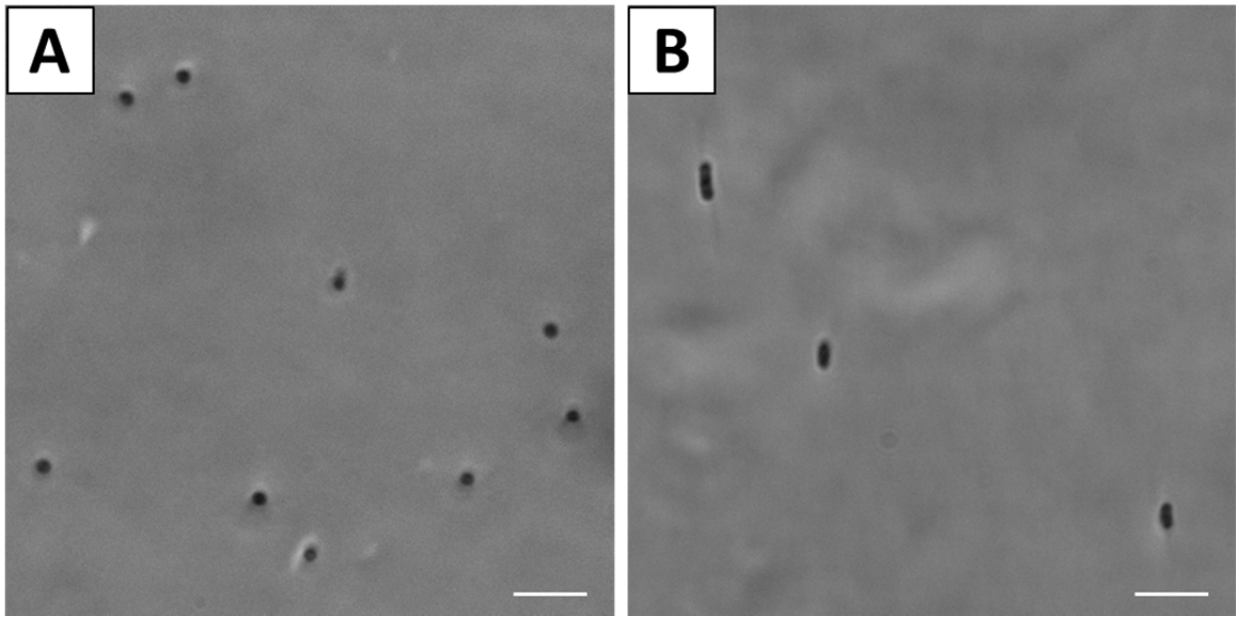

Fig. S4 Phase contrast microscopy images of vegetative *P. mirabilis* cells dispersed within a hybrid LC film (~ 18 μm thick) in a plane (A) near to the graphene-coated substrate and (B) near to the bare glass substrate. Scale bars = 5 μm.

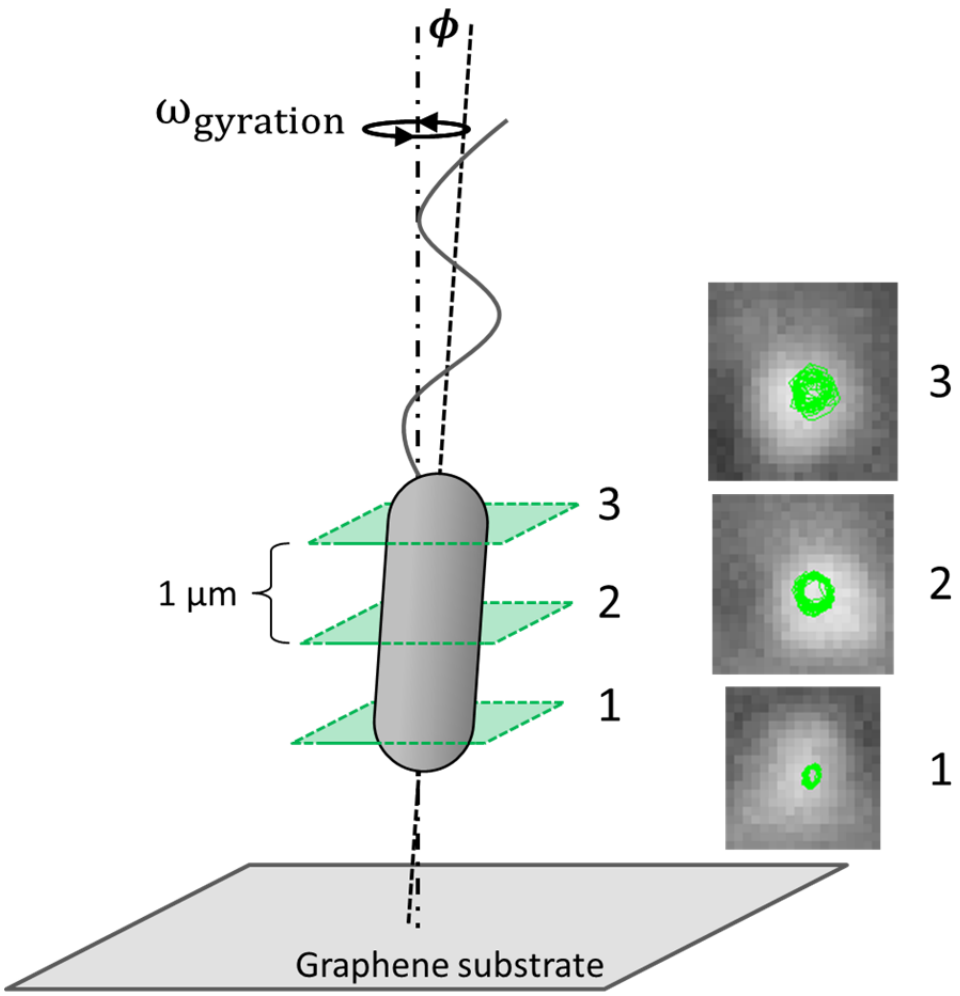

Fig. S5 Schematic and representative trajectories (each 200 frames long) collected at different planes of focus (each separated by 1 µm) of a gyrating vegetative cell near a graphene-coated substrate within a hybrid DSCG film.

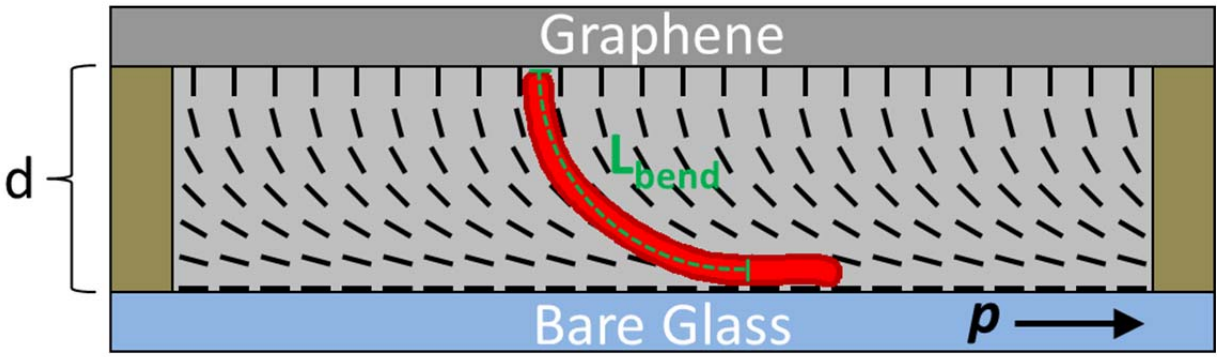

Fig. S6 Schematic depicting the configuration adopted by a swarm cell in a thin hybrid LC film in the limit of L > d.

Video Captions

Video S1 Phase contrast microscopy video of the motion of vegetative *P. mirabilis* cells dispersed in isotropic aqueous motility buffer between glass substrates in a cavity ~10 um thick.

Video S2 Phase contrast microscopy video of the motion of a vegetative *P. mirabilis* cell dispersed in a planar DSCG film created using two bare glass substrates. Due to the birefringence of the LC, distortions produced by the rotating flagella can be visualized in the wake of the bacterium.

Video S3 Phase contrast microscopy video of vegetative *P. mirabilis* cells dispersed in a uniform homeotropic DSCG film created using two graphene-coated substrates that orient parallel to the LC director (perpendicular to the graphene substrates). One cell is observed to move back and forth through the thickness of the LC film.

Video S4 Phase contrast microscopy video in which vegetative *P. mirabilis* cells in a uniform homeotropic DSCG film near one of the graphene substrates align approximately parallel to the far-field LC director and gyrate in tight circular trajectories (in a counterclockwise fashion when viewed from above the substrate) around an axis normal to the substrate.

Video S5 Phase contrast microscopy video in which a vegetative *P. mirabilis* cell in a uniform homeotropic DSCG film near one of the graphene substrates orients at a small angle with respect to the far-field LC director and gyrates in tight circular trajectories (in a counterclockwise fashion when viewed from above the substrate) around an axis normal to the substrate. Distortions in the LC induced by the rotating flagella bundle of the cell also can be observed.

Video S6 Phase contrast microscopy video of *P. mirabilis* swarm cells moving within a homeotropic DSCG film in directions orthogonal to the far-field director.

Video S7 Phase contrast microscopy video in which *P. mirabilis* swarm cells align and move parallel to the nematic director when dispersed in uniform planar DSCG films confined between bare glass slides.

Video S8 Phase contrast microscopy video of two motile *P. mirabilis* swarm cells moving within a homeotropic LC film. The transient strain in the LCs produced in the wake of one of the motile swarm cells leads to a change in the direction of motion of the second swarm cell.

Video S9 Phase contrast microscopy video (taken with a single polarizer inserted into the light path oriented in the vertical direction) of the motility of a *P. mirabilis* swarm cell within a homeotropic LC film and near to the graphene substrate farther from the objective. Viewed from above the graphene substrate, the cell appears to move in counterclockwise circles.

Video S10 Phase contrast microscopy video (taken with a single polarizer inserted into the light path oriented in the vertical direction) of the motility of a *P. mirabilis* swarm cell within a homeotropic LC film and near to the graphene substrate closer to the objective. Viewed from in front of the graphene substrate, the cell appears to move in clockwise circles.

Video S11 Phase contrast microscopy video showing rectification of the motion of a vegetative *P. mirabilis* cell in a hybrid LC film.

Video S12 Z-stack of images (phase contrast) of *P. mirabilis* swarm cells that have cell bodies that are extended through the thickness of a hybrid LC film.

Video S13 Phase contrast microscopy video of a vegetative *P. mirabilis* cell in a hybrid DSCG film positioned near the graphene substrate. The cell aligns approximately parallel to the local LC director and moves in tight circular trajectories (in a clockwise fashion when viewed from in front of the substrate) around an axis perpendicular to the substrate. Distortions in the LC induced by the rotating flagella bundle of the cell, which bends through the thickness of the LC film, also can be observed.